J-7-4

Extended Abstracts of the 2011 International Conference on Solid State Devices and Materials, Nagoya, 2011, pp1235-1236

Effect of Free Carriers on Dopant-induced Surface Potential in SOI-FETs

Miftahul Anwar,[1] Roland Nowak,[1,2] Daniel Moraru,[1] Ryszard Jablonski,[2]
Takeshi Mizuno,[1] and Michiharu Tabe[1]

[1]Research Institute of Electronics, Shizuoka University, 3-5-1 Johoku Hamamatsu 432-8011, Japan
TEL/FAX: +81-53-478-1335; e-mail: miftah_war@rie.shizuoka.ac.jp
[2]Division of Sensors and Measuring Systems, Faculty of Mechatronics, Warsaw University of Technology, Poland

1. Introduction

In the last decade, innovative applications, such as quantum computing [1] and single-dopant FETs [2-4], based on single dopants in silicon, have been proposed. In study of dopant devices, it is crucial to measure location and potential of a single dopant atom. One of the most powerful tools for this purpose is Kelvin Probe Force Microscopy (KFM) [5], which can detect local electrostatic force on the surface. We reported single dopant observation in SOI-FETs by the KFM technique at low temperatures [6], as well as electron charging in dopants and clusters of dopants [7].

In this work, we study interplay of free carriers with dopants in KFM potential images. Differences between measurements at low and room temperature are presented. At low temperature, the effect of free carriers on potential is important only at positive voltages, while at room temperature it is significant in whole range of applied voltages.

2. Separation of free carriers by internal electric field

Experimental setup of the KFM measurement is schematically shown in Fig. 1. A grounded metallic cantilever scans over the device surface at constant height. Backgate voltage, V_{BG}, is used to modulate potential within the channel region. A dc-voltage (not shown), applied in order to nullify electrostatic force between tip and sample, corresponds to the actual value of electronic potential.

We fabricated and studied silicon-on-insulator (SOI) FETs, as schematically shown in Fig. 1. The top 10-nm-thick Si layer was doped with phosphorus ($N_D \approx 1 \times 10^{18}$ cm^{-3}, i.e., the average inter-dopant distance of 10 nm). The channel surface is covered with a thin (2 nm) SiO_2 layer that was grown by dry oxidation.

First, we measured channel potential at low temperature (14 K). Source and drain electrodes were grounded, while backgate voltage (V_{BG}) was changing from -4 to +4 V with 1 V step. Figure 2(a) shows obtained topography image and Figs. 2(b)-(d) show potential images for -4, 0 and +4 V, respectively. As it can be seen, the potential contrast successively becomes smaller with increasing V_{BG} and eventually disappears at +4 V. In Fig. 4(a), the root mean square (RMS) of the potential is presented as a measure of contrast. The blue curve indicates gradual contrast weakening at low temperature. Figure 4(b) shows schematic sketch of device cross-sectional view at +4 V in a low temperature condition. Dopants (P atoms) are mainly located in the depressed regions of the surface, which is due to the dependence of the oxidation process on the presence of dopants. By applying negative V_{BG}, the channel is depleted and, accordingly, the obtained potential image is mainly due to positively-charged donors. This mechanism explains the similarity between topography and potential map at -4 V. With increasing V_{BG}, free electrons are injected into the channel region (from source and drain pads) and screen the dopants. This effect, illustrated in Fig. 4(b), causes the potential contrast to disappear, as seen in Fig. 2(d).

For room temperature measurements, the procedure is similar. Figure 3(a) shows obtained topography image and Figs. 3 (b)-(d) show potential images for -4, 0 and +4 V, respectively. At room temperature (300 K), however, due to the thermal activation, the number of free carriers becomes large. Once an electron-hole pair is created, internal electric field across the device will separate electrons and holes, as shown in Fig. 4(c). For negative V_{BG}'s, holes are attracted towards Si/buried oxide interface, whereas electrons are repelled towards protruded surface regions. This spatial charge separation is responsible for the similar contrast between topography [Fig. 3(a)] and potential maps [Fig. 3(b)]. For positive V_{BG} range, on the other hand, situation will be opposite. In this case, electrons are attracted towards the Si/buried oxide interface and holes are pushed out towards the protruded areas, as shown in Fig. 4(c). It results in opposite contrast between topography [Fig. 3(a)] and potential image [Fig. 3(d)].

The behavior of the contrast, from negative to positive V_{BG}'s, is also illustrated in Fig. 4(a) by the red curve. The trend on the left-side branch ("similar contrast") corresponds to gradual potential contrast reduction. When V_{BG} approaches 0 V, thermally-activated carrier separation becomes weaker. At around 0 V, the curve reaches its minimum, indicating lowest potential contrast, as seen in Fig. 3(c). In this case, the dominant effect is due to screening by free electrons, distributed within the whole channel region. The right-side branch, with increasing trend ("opposite contrast"), is related to hole accumulation in the protruded surface regions, as seen in Fig. 3(d).

3. Conclusions

We showed significant difference between KFM maps at low and room temperature. At low temperatures, the effect of free carriers is important only at positive backgate voltages, while at room temperature, it is important in the whole range of applied V_{BG}. This result is essential for clarifying the interaction between dopants and free carriers.

Acknowledgements
This work was partially supported by KAKENHI (20246060 and 22656082).

References

[1] B. E. Kane, Nature **393**, 133 (1998).
[2] M. Tabe *et al.*, Phys. Rev. Lett., **105**, 016803 (2010).
[3] H. Sellier *et al.*, Phys. Rev. Lett. **97**, 206805 (2006).
[4] Y. Ono *et al.*, Appl. Phys. Lett. **90**, 10216 (2007).
[5] M. Nonnenmacher *et al.*, Appl. Phys. Lett. **58**, 2921 (1991).
[6] M. Ligowski *et al.*, Appl. Phys. Lett. **93**, 142101 (2008).
[7] M. Anwar *et al.*, Jpn. J. Appl. Phys., to be published (2011).

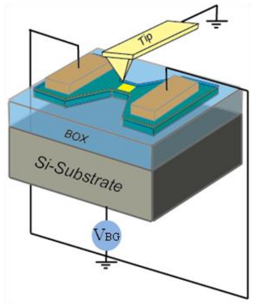

FIG. 1. SOI-FET under KFM measurement: schematic device structure and setup.

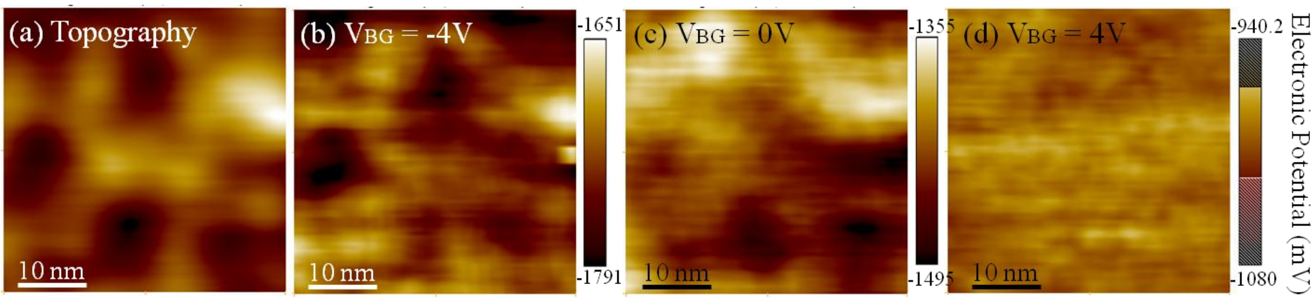

FIG. 2. Results at 14K: (a) topography image; (b)-(d) potential images. At -4 V, the contrasts of topography [(a)] and KFM [(b)] are similar, while, with increasing voltages, the KFM images become flat due to injection of electrons and resultant screening effect.

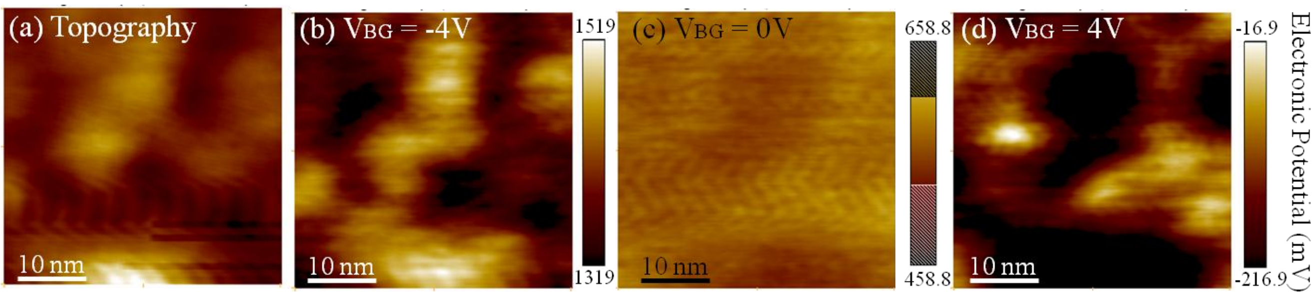

FIG. 3. Results at room temperature: (a) topography image; (b)-(d) potential images. For -4 V, topography [(a)] and KFM [(b)] are similar due to electron accumulation in protruded regions. At 0 V [(c)], the contrast of KFM image disappears because of screening effect. Finally, at +4 V [(d)], the KFM image and topography [(a)] exhibit opposite contrasts due to hole accumulation in the protruded regions of the surface.

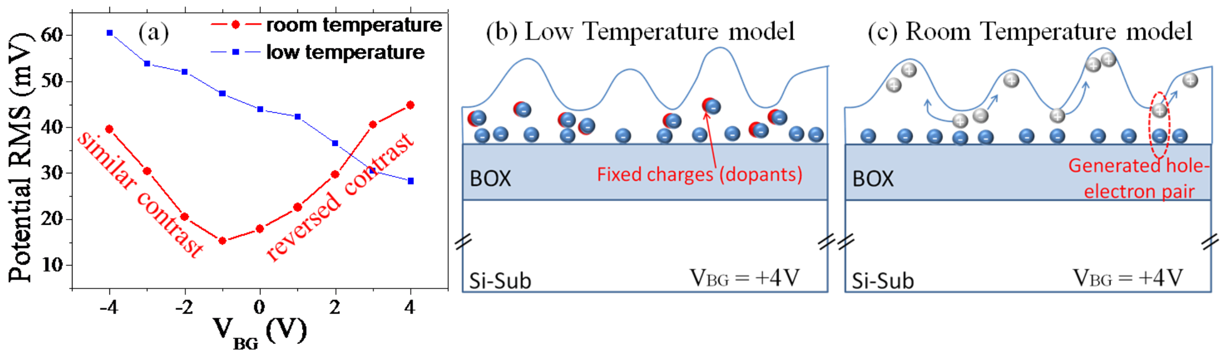

FIG. 4. (a) RMS (relative contrast) of KFM images *vs.* V_{BG} taken at room temperature (the red curve) and a low temperature, 14K, (the blue curve). The monotonous decrease of RMS at 14K with increasing V_{BG} is ascribed to individual dopant observation and then screening of dopant potential due to successive injection of electrons, as indicated in (b). In contrast, RMS at RT is decreasing with increasing V_{BG} first, and then increasing. This behavior is primarily ascribed to separation of free carriers (electrons and holes). In (c), a schematic view of holes and electrons at +4 V is shown, where holes are gathering in protruded surface regions.